International Journal of Power Electronics and Drive System (IJPEDS)
Vol. 8, No. 2, June 2017, pp. 548~557
ISSN: 2088-8694, DOI: 10.11591/ijpeds.v8i2.pp548-557

Novel Compensation Method to Reduce Rotor Position Estimation Error and Torque Reduction in Signal Injection Based PMSM Drives

Ravikumar Setty Allampalli[1], Purna Prajna R Mangsuli[2], Kishore Chatterjee[3]
[1,2] Honeywell Technology Solutions, Bangalore, India
[3] Electrical Engineering Department, IIT Bombay, Mumbai, India

Article Info

Article history:

Received Jan 4, 2017
Revised Mar 4, 2017
Accepted Mar 24, 2017

Keyword:

High frequency signal injection
Permanent Magnet
Synchronous Motor
Position estimation error
Self-sensing techniques
Stator winding resistance

ABSTRACT

High frequency signal injection techniques are widely used to extract rotor position information from low speed to stand still. Accuracy of estimated rotor position is decreased when stator winding resistance is neglected. Position estimation error also results in output Torque reduction. Parasitic resistance of stator winding causes significant position estimation error and Torque reduction, if not compensated. Signal injection techniques developed in the literature does not provide detailed analysis and compensation methods to improve rotor position estimation of PMS Motors, where stator winding resistance cannot be neglected. This work analyzes the stator winding resistance effect on position estimation accuracy and proposes novel compensation technique to reduce the position estimation error and torque reduction introduced by stator winding resistance. Prototype hardware of a self-sensing PMSM drive is developed. The effectiveness of the proposed method is verified with the MATLAB/Simulink simulations and experimental results on a prototype self-sensing PMSM drive.

Corresponding Author:

Ravikumar Setty Allampalli,
Honeywell Technology Solutions,
Adarsh Prime Project Pvt Ltd,
Survey No 19/2, Devarabisanahalli Village,
K.R. Puram Hobli, Bangalore -560 103, India.
Email: arksetty@iitb.ac.in

NOMENCLATURE

R	Stator winding resistance / Phase
L	Stator winding inductance / Phase
L_d, L_q	Stator winding inductance of direct and quadrature axis components
αβ	Stator orthogonal coordinate system
dq	Rotor orthogonal coordinate system
dq'	Magnetic axis referred on rotor side
A	3 phase to 2 phase transformation matrix (Clark Transformation)
B	αβ to dq transformation matrix (Park Transformation)
T	Transpose
v_c, i_c	High frequency voltage and high frequency current response
L_c	High frequency stator inductance vector
PMSM	Permanent Magnet Synchronous Motor
V_{DC}	DC Supply Voltage to Inverter
I_a,I_b,I_c	Currents through Phase a, b and c respectively

i_{cp}, i_{cn}	Positive and Negative sequence components of carrier current response
Ψ_{cp}, Ψ_{cn}	Phase of Positive and Negative sequence carrier currents
$\boldsymbol{\lambda_{dq}}$	Rotor Magnetic saliency Position angle

1. INTRODUCTION

Permanent Magnet Synchronous Motors (PMSM) are increasingly used in high performance applications. This is because PMS motor has many advantages, like high efficiency, high torque to inertia ratio, rapid dynamic response, and maintenance-free operation [1]. Rotor position information is required to control PMS motor. Extracting rotor position information using position sensor presents several disadvantages, including increased size, reduced reliability, and additional cost of the position sensor [2]. To overcome these drawbacks, there has been considerable interest in self-sensing or sensor less control techniques. The key problem in sensor less control of PMS motor drives is the accurate estimation of the rotor position over a wide speed range using only terminal variables [2]-[3].

Sensor less control techniques uses only terminal variables (voltages and currents) to determine the rotor position. Back EMF based techniques are well proven and popular to extract rotor position information from medium to high speeds [4]. Several techniques are proposed based on sliding mode control using back EMF information, however all these techniques works well above minimum speed and fail to extract the rotor position from low speed to standstill [5]-[6].

At standstill, motor back EMF is zero, so all fundamental methods based on back EMF fail to extract rotor position information. From low speed to standstill machine saliency is used to estimate rotor position information. Magnetic saliency based sensor less control techniques are widely used due to their robustness at low speed to standstill [7]. In order to estimate the rotor position from machine saliency, specific high frequency signal is injected and high frequency current response is demodulated to derive the rotor position. According to the type of signal injected, signal injection techniques are classified into Rotating Frequency Injection (RFI) and Pulsating Frequency Injection (PFI). High frequency carrier signal rotating at a frequency (500-1500Hz) is superimposed on the fundamental voltage vector and resuting carrier current response is used to extract the rotor position. Increasing the injected signal frequency affect the current control loop bandwidths [8]-[9].

Pulsating injection is based on an alternating carrier signal injection that oscillates in either d-axis or q-axis and resulting carrier current response provide the rotor position information [10]-[11]. Advantages and disadvantages of rotating and pulsating voltage injection techniques are addressed in [12]-[13], and both the techniques are widely accepted for the position estimation from low speed to stand still.

Even though signal injection techniques are widely accepted for the rotor position estimation from low speed to standstill, Position estimation accuracy of these techniques is affected by many sources of error. Inverter non linearity due to dead time, introduction of delays due to filtering, not accounting stator winding resistance and cross saturation effects results in significant position estimation error [14]. Many solutions are proposed and validated for compensating the dead time effect and other inverter nonlinearities [15]-[16]. Work performed in [17] adds cross saturation component to the input of position observer, which helps in improving the Position estimation accuracy due to cross saturation.

Work performed in [18] uses positive sequence and negative sequence currents to reduce position estimation error due to stator winding resistance and measurement delays. This method require large high frequency signal amplitude to extract negative sequence currents. Large signal amplitudes increase the torque ripple and audible noise [19]-[20]. Use adaptive observer to estimate the stator resistance. Observer is designed with high frequency signal injection technique at low speeds and same is used for the adaptation of the motor parameters to reduce the rotor position estimation error. This work explained about the measurement of stator resistance but does not provide any compensation to improve the estimation accuracy. Work performed in [21] improve the rotor position estimation accuracy utilizing zero-sequence carrier voltage, but this method require additional voltage sensor [22]. Improve the Position estimation accuracy, but this method requires additional low cost hall sensors. Usage of hall sensors reduce the reliability of the drive and limit the operation to non- harsh environments.

Proposed work analyzes the effect of stator winding resistance on position estimation error and proposes compensation technique to minimize this error in rotating signal injection based techniques. Analytical expressions are derived for position estimation error when stator winding resistance is neglected. This error component is used to improve the position estimation accuracy. This work also shows decrease in torque reduction when stator winding resistance is considered for position estimation. Finally proposed compensation method is simulated using MATLAB/Simulink and same is validated using Prototype PMSM drive based on rotating high frequency signal injection technique.

2. PROPOSED COMPENSATION METHOD TO REDUCE POSITION ESTIMATION ERROR

Position sensor less techniques based on High Frequency (HF) signal injection superimpose additional HF signal on fundamental component. Current response to the Injected HF carrier voltage is used to extract the Rotor Position Angle. From (4) it can be seen that the resulting HF current contains two rotating vector components. One component rotating in the same direction (Positive Sequence) and one rotating in the opposite direction (Negative Sequence) to the injected HF voltage. Negative sequence component contains rotor position information and this component is demodulated to extract rotor position. Phase angle of negative sequence component (ψ_{cn}) shown in (6) contains stator winding resistance. Estimation error increases when the voltage drop across the winding resistance is comparable to winding reactance. Permanent magnet motors used in the servo application have much smaller winding inductances [23]-[24], so at the injection frequency voltage drop across the winding resistance is comparable to winding reactance. Neglecting the winding resistance results in significant position estimation error and Torque reduction.

Rotor position estimation using rotating high frequency signal injection is shown in Figure 1. Rotating high frequency signal is injected in the αβ -reference frame. A rotating HF current vector arises superimposed to the fundamental current vector. The high frequency current response is filtered out by a band pass filter (BPF) from the measured machine currents and then demodulated to reconstruct the rotor position. The same measured phase currents are used as feedback for the fundamental current controllers after the injected HF currents are filtered off by a low or band stop filter (BSF). Various demodulation techniques [25] are proposed in the literature, this work uses hetero dyne demodulation technique to extract the rotor position from high frequency current response. VSI operates at 10 kHz switching frequency with ~2uS dead time, average voltage loss over one PWM cycle due to dead time, is compensated by adding the lost volts- secs to the reference voltage to get the desired output voltage.

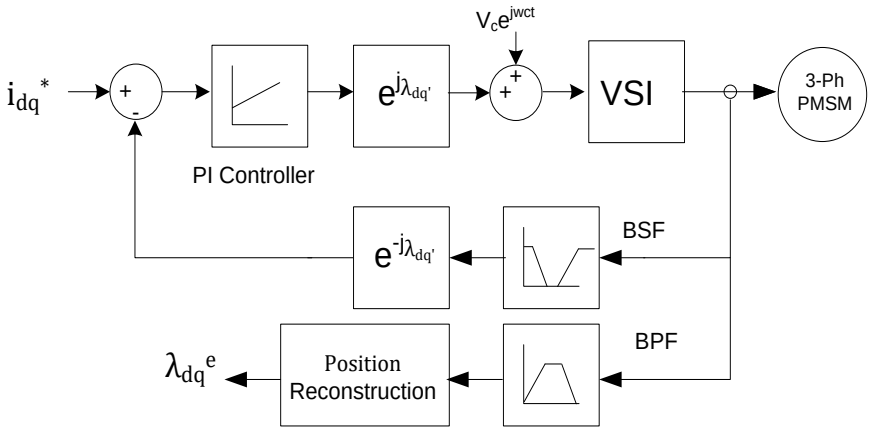

Figure 1. Block diagram of rotating HF voltage carrier injection.

Conventional rotating HF voltage carrier injection techniques [8]-[9] doesn't consider the stator winding resistance in to the rotor position estimation. When stator winding resistance is neglected, ψ_{cn} becomes zero, which results in rotor position estimation error. Proposed compensation technique derives(ψ_{cn}) component as shown in (7), which accounts for position estimation error due to stator winding resistance. This term is used to derive the compensated rotor position information. Functional block diagram of the rotor position estimation with stator winding resistance compensation is shown in Figure 2.

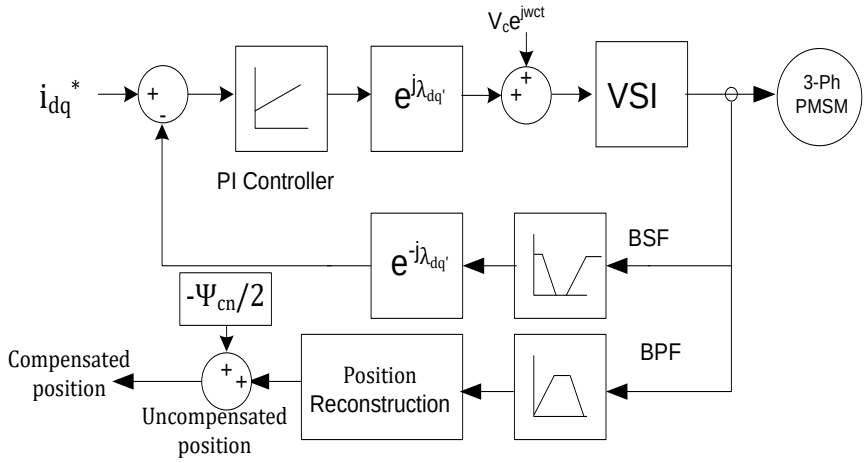

Figure 2. Proposed Compensation method to reduce position estimation error due to stator winding resistance.

3. MATHEMATICAL ANALYSIS OF POSITION ESTIMATION ERROR DUE TO STATOR WINDING RESISTANCE

High frequency model of PMSM considering stator winding resistance can be represented by (1).

$$\overrightarrow{v_c} = R\,\overrightarrow{i_c} + L_c\frac{d\overrightarrow{i_c}}{dt} \tag{1}$$

$$\begin{bmatrix} v_{cd'} \\ v_{cq'} \end{bmatrix} = \begin{bmatrix} R & 0 \\ 0 & R \end{bmatrix}\begin{bmatrix} i_{cd'} \\ i_{cq'} \end{bmatrix} + \begin{bmatrix} L_c - \left[\frac{\Delta L_c}{2}\right] & 0 \\ 0 & L_c + \left[\frac{\Delta L_c}{2}\right] \end{bmatrix} x \frac{d}{dt}\begin{bmatrix} i_{cd'} \\ i_{cq'} \end{bmatrix} \tag{2}$$

Equation (3) shows the transformation into the stator fixed αβ frame.

$$\begin{bmatrix} v_{c\alpha} \\ v_{c\beta} \end{bmatrix} = R\begin{bmatrix} i_{c\alpha} \\ i_{c\beta} \end{bmatrix} + \begin{bmatrix} L_c - \left[\frac{\Delta L_c}{2} * \cos\left(2\lambda_{dq'}\right)\right] & -\left[\frac{\Delta L_c}{2} * \sin\left(2\lambda_{dq'}\right)\right] \\ -\left[\frac{\Delta L_c}{2} * \sin\left(2\lambda_{dq'}\right)\right] & L_c + \left[\frac{\Delta L_c}{2} * \cos\left(2\lambda_{dq'}\right)\right] \end{bmatrix} x \frac{d}{dt}\begin{bmatrix} i_{c\alpha} \\ i_{c\beta} \end{bmatrix} \tag{3}$$

Solving above differential Equations $\overrightarrow{i_{c\alpha\beta}}$ can be expressed as

$$\overrightarrow{i_{c\alpha\beta}} = \left(i_{cp} e^{j\left(w_c t - \frac{\pi}{2} + \psi_{cp}\right)}\right) + \left(i_{cn}\, e^{-j\left(w_c t - 2\lambda_{dq'} - \pi/2 + \psi_{cn}\right)}\right) \tag{4}$$

Where

$$i_{cp} = \frac{V_c}{2}\sqrt{\left[\frac{w_c\left(L_c - \left[\frac{\Delta L_c}{2}\right]\right)}{R^2 + \left(w_c\left(L_c - \left[\frac{\Delta L_c}{2}\right]\right)\right)^2} + \frac{w_c\left(L_c + \left[\frac{\Delta L_c}{2}\right]\right)}{R^2 + \left(w_c\left(L_c + \left[\frac{\Delta L_c}{2}\right]\right)\right)^2}\right]^2 + \left[\frac{R}{R^2 + \left(w_c\left(L_c - \left[\frac{\Delta L_c}{2}\right]\right)\right)^2} + \frac{R}{R^2 + \left(w_c\left(L_c + \left[\frac{\Delta L_c}{2}\right]\right)\right)^2}\right]^2}$$

$$i_{cn} = \frac{V_c}{2}\sqrt{\left[\frac{w_c\left(L_c - \left[\frac{\Delta L_c}{2}\right]\right)}{R^2 + \left(w_c\left(L_c - \left[\frac{\Delta L_c}{2}\right]\right)\right)^2} - \frac{w_c\left(L_c + \left[\frac{\Delta L_c}{2}\right]\right)}{R^2 + \left(w_c\left(L_c + \left[\frac{\Delta L_c}{2}\right]\right)\right)^2}\right]^2 + \left[\frac{R}{R^2 + \left(w_c\left(L_c - \left[\frac{\Delta L_c}{2}\right]\right)\right)^2} - \frac{R}{R^2 + \left(w_c\left(L_c + \left[\frac{\Delta L_c}{2}\right]\right)\right)^2}\right]^2} \tag{5}$$

$$\psi_{cp} = tan^{-1}\left(\frac{\left[\frac{R}{R^2+\left(w_c\left(L_c-\left[\frac{\Delta L_c}{2}\right]\right)\right)^2}+\frac{R}{R^2+\left(w_c\left(L_c+\left[\frac{\Delta L_c}{2}\right]\right)\right)^2}\right]}{\left[\frac{w_c\left(L_c-\left[\frac{\Delta L_c}{2}\right]\right)}{R^2+\left(w_c\left(L_c-\left[\frac{\Delta L_c}{2}\right]\right)\right)^2}+\frac{w_c\left(L_c+\left[\frac{\Delta L_c}{2}\right]\right)}{R^2+\left(w_c\left(L_c+\left[\frac{\Delta L_c}{2}\right]\right)\right)^2}\right]}\right) \psi_{cn} = tan^{-1}\left(\frac{\left[\frac{R}{R^2+\left(w_c\left(L_c-\left[\frac{\Delta L_c}{2}\right]\right)\right)^2}-\frac{R}{R^2+\left(w_c\left(L_c+\left[\frac{\Delta L_c}{2}\right]\right)\right)^2}\right]}{\left[\frac{w_c\left(L_c-\left[\frac{\Delta L_c}{2}\right]\right)}{R^2+\left(w_c\left(L_c-\left[\frac{\Delta L_c}{2}\right]\right)\right)^2}-\frac{w_c\left(L_c+\left[\frac{\Delta L_c}{2}\right]\right)}{R^2+\left(w_c\left(L_c+\left[\frac{\Delta L_c}{2}\right]\right)\right)^2}\right]}\right) \quad (6)$$

From (4) it can be seen that the resulting HF current contains two rotating vector components. One component is rotating with the injected voltage frequency in the same direction and one rotating at $(-w_c t + 2\,\lambda_{dq'} + \frac{\pi}{2} - \psi_{cn})$ in the opposite direction to the injected HF voltage. ψ_{cn} Component shown in (6) accounts stator winding resistance in calculations [26].

Assuming $w_c{}^3 * \left(L_c + \left[\frac{\Delta L_c}{2}\right]\right) * \left(L_c - \left[\frac{\Delta L_c}{2}\right]\right) * \left(L_c + \left[\frac{\Delta L_c}{2}\right]\right) - \left(L_c - \left[\frac{\Delta L_c}{2}\right]\right) >>$

$$w_c * R^2 * \left(L_c + \left[\frac{\Delta L_c}{2}\right]\right) - \left(L_c - \left[\frac{\Delta L_c}{2}\right]\right)$$

ψ_{cn} Can be simplified to

$$\psi_{cn} = tan^{-1}\left(\frac{[2RL_c]}{\left[w_c*\left(L_c+\left[\frac{\Delta L_c}{2}\right]\right)*\left(L_c-\left[\frac{\Delta L_c}{2}\right]\right)\right]}\right) \quad (7)$$

With the demodulation approach shown in Figure 3 ε can be expressed as

$$\varepsilon = i_{cp} sin\left(2w_c t - 2\lambda_{dq'} e + \psi_{cp}\right) + i_{cn} sin\left(2\lambda_{dq'} - 2\lambda_{dq'} e + \psi_{cn}\right) \quad (8)$$

When ϵ passed through low pass filter, first term gets filtered out and PI controller adjusts $(2\lambda_{dq'} - 2\lambda_{dq'} e + \psi_{cn})$ to zero. Error between actual and estimated position is expressed as

$$\lambda_{dq'} - \lambda_{dq'} e \;=\; -\psi_{cn}/2 = -\frac{tan^{-1}\left(\frac{[2RL_c]}{\left[w_c*\left(L_c+\left[\frac{\Delta L_c}{2}\right]\right)*\left(L_c-\left[\frac{\Delta L_c}{2}\right]\right)\right]}\right)}{2} \quad (9)$$

Equation (9) shows the error introduced in rotor position estimation when stator winding resistance neglected. This term (9) is added to estimated rotor position to compensate for the stator winding resistance error.

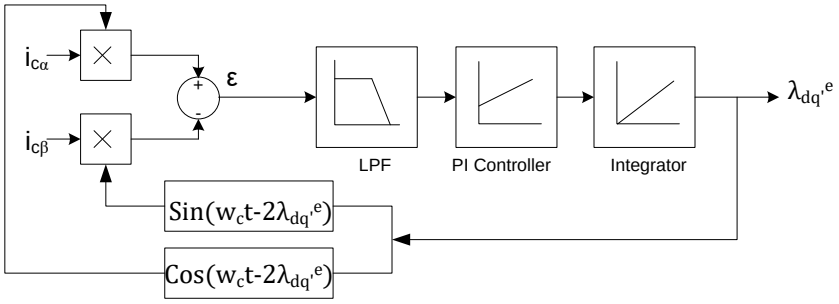

Figure 3. Hetero dyne observer using PI Controller to track rotor position

4. RESULTS AND CONCLUSION

4.1. Analysis and Simulation Results

Detailed Mathematical analysis is carried to study the Position estimation error due to stator winding resistance and error is calculated using (9). Two motors with different winding resistance are selected. Selected motor parameters and calculated position estimation errors are shown in Table 1.

Table 1. Calculated Position Estimation Error

	Motor Series	R(ohms)	Lc(mH)	Rated Speed (RPM)	Rated Torque (Nm)	Rated Power (kW)	Injected Signal Freq. (Hz)	Calculated Error(Deg)
Motor-1	HJ96c6	1.6	3.5	4500	2.6	1.2	500	8.43
Motor-2	AKM21	3.42	5.2	2500	0.46	0.32	500	11.78

After the mathematical analysis, detailed simulation of the proposed compensation method is carried using MATLAB/Simulink platform. Figure 4 shows the sensor less position estimation based on RFI. Starting from top, waveform order is Rotating HF signal, Motor speed, Estimated and Actual Rotor Position and Error between the estimated and actual rotor positions. This simulation result validate the RFI modelling.

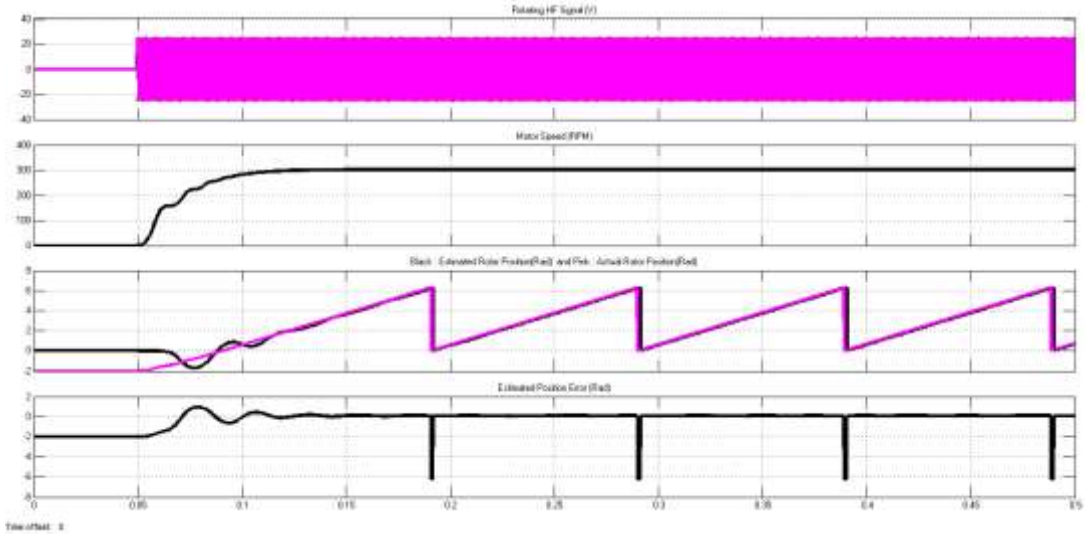

Figure 4. Motor-1 Sensor less Position Estimation Results (Before Compensation)

Figure 5 clearly shows the effect of stator winding resistance on position estimation error. From the simulation results position estimation error before compensation is 9 Deg and 14 Deg respectively on Motor-1 and 2. Using proposed compensation position estimation error is reduced to 4 Deg as shown Figure 6.

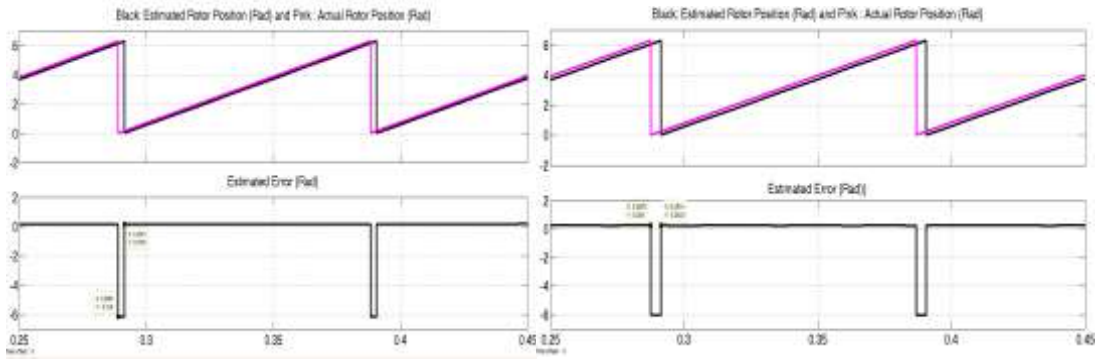

(a) (b)

Figure 5. (a) Motor-1 Position Estimation Error before compensation (b) Motor-2 Position Estimation Error before compensation

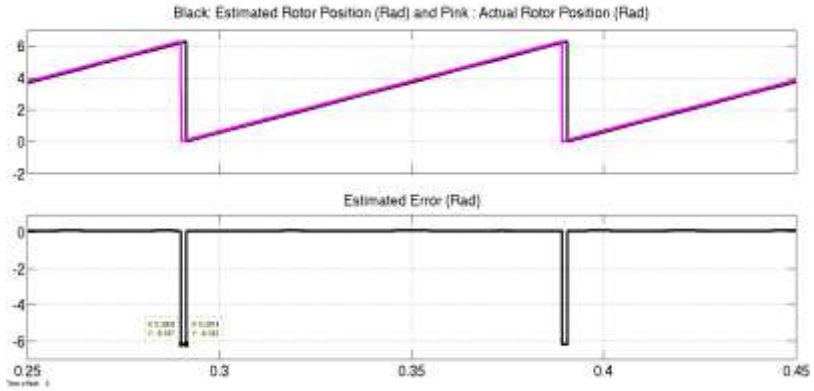

Figure 6. Motor-1 and Motor-2 Position Estimation Error using Proposed Compensation Method

4.2 Experimental Results

Simulation results clearly shows the proposed compensation method reduce the position estimation error up to 5 Deg on Motor-1 and 10 Deg on Motor-2. Which is now validated using experimentation. Experimental set up block diagram and hardware pictures are shown in Figure 7 and Figure 8. Description of the equipment used is listed in Table 2.

Table 2. Major equipment used in the hardware setup

Equipment	Description
Motor	3 phase PMSM. Table-1 shows the Motor parameters
Inverter	3 phase six switch inverter, 4A/400V.
Controller	Texas Instruments TMS320F28035
Power supply	Inverter :100 VDC Logic Circuit: 3.3 VDC Gate Driver : 15 VDC
Resolver Power Supply	11Vrms and 8kHz ac signal.

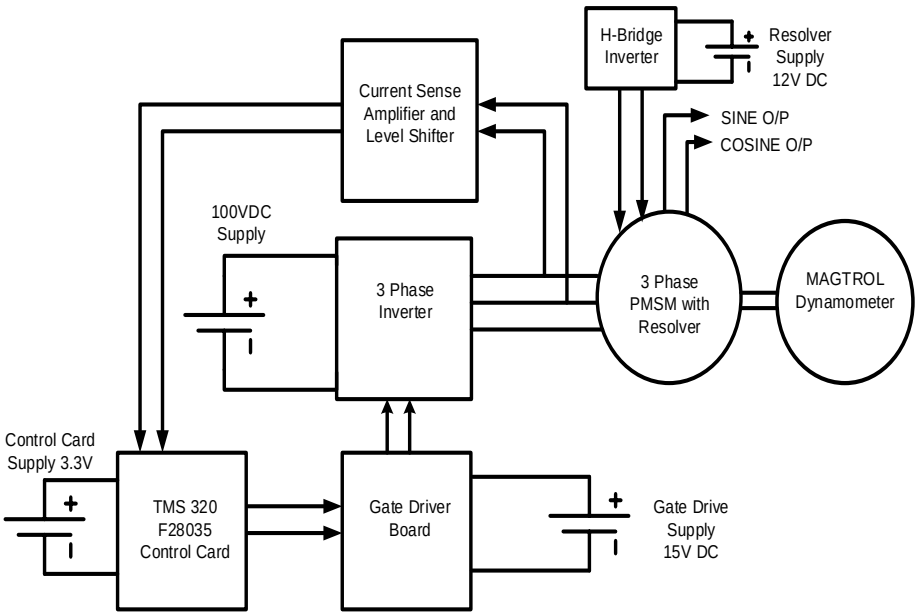

Figure 7. Hardware set-up High level block diagram.

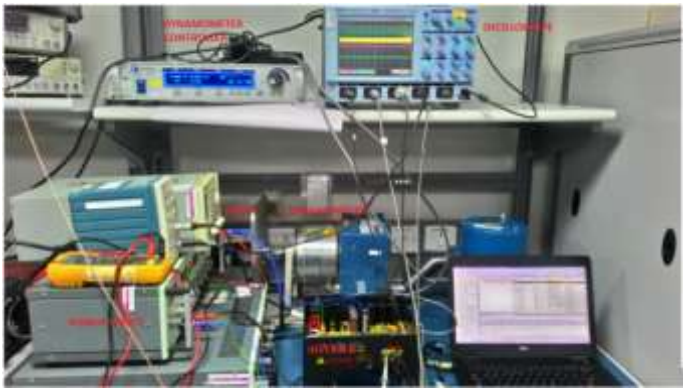

Figure 8. Experimental setup used to study the Proposed Compensation Method

Rotor position estimation results using RFI is shown in Figure 9. Current response to the injected signal contains rotor position and polarity detection is determined using [14]. Estimated rotor position track with the resolver output. Figure 9 show the traces of Resolver Sine output, Estimated Rotor position, HF current and motor phase current.

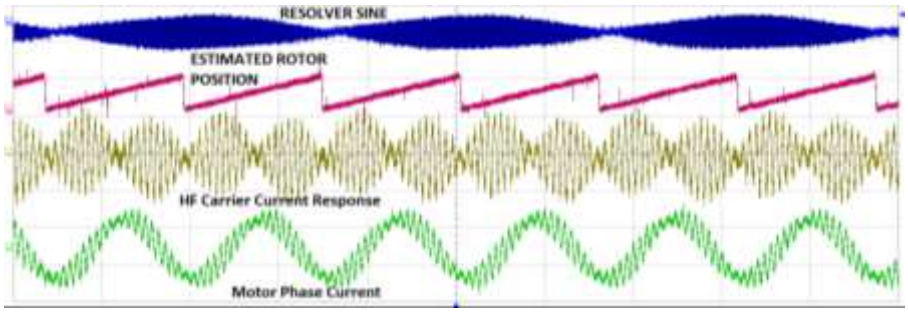

Figure 9. Estimated Rotor Position Comparison with resolver output on Motor-1 before compensation.

After establishing and verifying the sensor less position estimation using RFI. Proposed compensation method is applied to study the position estimation error on Motor -1 and Motor -2. Figure 10 and Figure 11 compare the position estimation error before and after proposed compensation on Motor-1 and Motor-2 respectively. Proposed compensation method reduce the position estimation error from 10 Deg. to 5 Deg. and % Torque reduction from 1.51 to 0.38 on Motor-1. On Motor-2 position estimation error is reduced from 16 Deg. to 5 Deg. and % Torque reduction from 3.87 to 0.38.

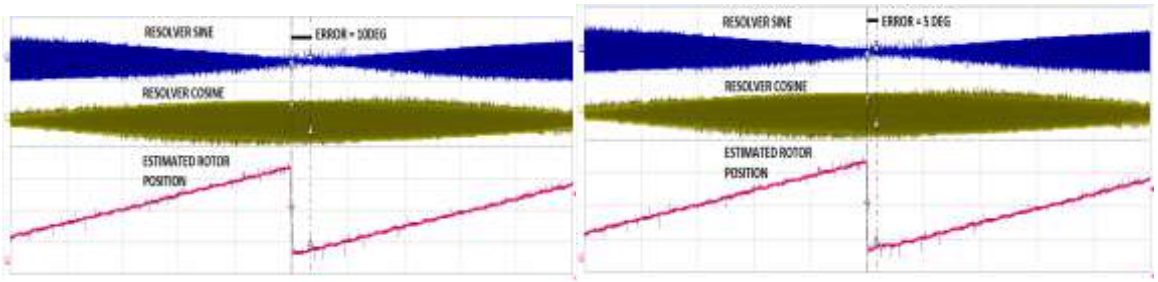

(a) (b)

Figure 10. Estimated Rotor Position Comparison with resolver output on Motor-1 (a) before compensation (b) after compensation

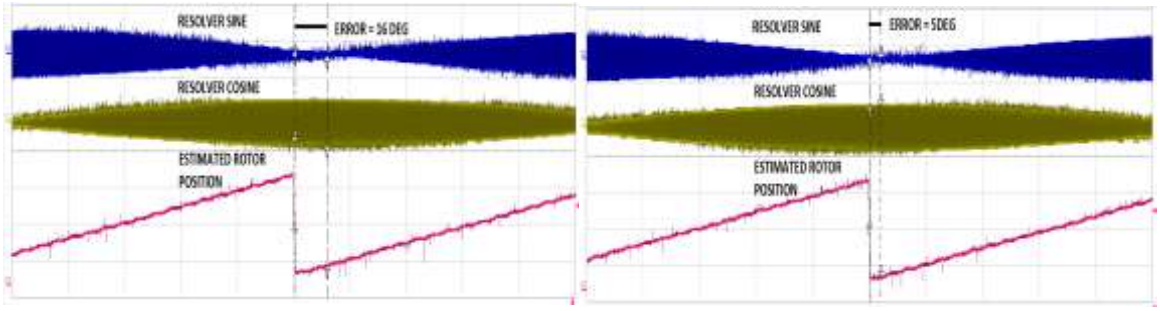

(a) (b)

Figure 11. Estimated Rotor Position Comparison with resolver output on Motor-2 (a) before compensation (b) after compensation

Comparison between the conventional RFI method where stator winding resistor is not accounted and proposed method with considering stator winding resistance is shown in Table-3. Motor-2 take higher benefit compared to Motor-1 because the uncompensated error is large. For the applications where stator winding resistance is not negligible, proposed compensation method significantly reduce the position estimation error and reduction in output torque.

Table 3. Position Estimation Error and Torque Reduction comparison between Conventional Method and Proposed Compensation Method

Method of Control		Position Estimation error from Simulation Result (Deg)	Error reduction using Proposed Compensation Simulation Result (Deg)	Position Estimation error from Board Measurements (Deg)	Error reduction using Proposed Compensation Experimental Result (Deg)	Torque Reduction (%)	Decrease In the Torque Reduction with Proposed Compensation (%)
Motor-1	Conventional Method	9	5	10	5	1.51	1.13
	Proposed Compensation	4		5		0.38	
Motor-2	Conventional Method	14	10	16	11	3.87	3.49
	Proposed Compensation	4		5		0.38	

5. CONCLUSION

This work aim to improve the performance of PMSM drives based on high frequency signal injection technique, where the stator winding resistance cannot be neglected. Presented detailed analysis, simulation and experimentation results to show the effect of stator winding resistance on position estimation error. From the simulation and experimental results it is evident that impact of estimation error depends on the motor parameters. Where the estimation error due to winding resistance is significant, proposed compensation method effectively reduce the error. Two motors with different winding resistance and inductance are selected to validate the proposed compensation method. Proposed compensation method effectively reduced the estimation error and torque reduction due to stator winding resistance. Efficacy of the proposed method is verified using detailed simulation results. The viability of the proposed scheme is validated using experimental results.

REFERENCES

[1] K. Rajashekara, *et al.*, "Sensorless Control of AC Motor Drives, Speed and Position Sensorless Operation" IEEE Press, 1996.
[2] P. P. Acarnley and J. F. Watson, "Review of position-sensorless operation of brushless permanent-magnet machines," *IEEE Trans. Ind. Electron.*, vol.53, no.2, pp.352-362, 2006.
[3] T. Kim, *et al.*, "Position sensorless brushless DC motor/generator drives: Review and future trends," *IET Elect. Power Appl.*, vol.1, no.4, pp.557–564, Jul.2007.

[4] Gaolin Wang, et al., "DSP-Based Control of Sensorless IPMSM Drives for Wide-Speed-Range Operation," *IEEE Trans. Ind. Electron.,* vol.60, no.2,pp.720-727, 2013.
[5] Rachid Askour, et al., "DSP-Based Sensorless Speed Control of a Permanent Magnet Synchronous Motor using Sliding Mode Current Observer," *International Journal of Power Electronics and Drive Systems,*vol.4, no. 3,pp. 281-289, Sep.2014.
[6] Gouichiche Abdelmadjid, et al., "Sensorless Sliding Mode Vector Control of Induction Motor Drives" *International Journal of Power Electronics and Drive Systems,*vol. 2, no.3,pp.277-284,Sep.2012.
[7] H. Kim and R.D. Lorenz, "Carrier signal injection based sensorless control methods for IPM synchronous machine drives," *IEEE-IAS Annual Meeting,* vol. 2, pp.977-984, Oct.2004.
[8] P. Garcia, et al., "Accuracy, bandwidth, and stability limits of carrier-signal-injection-based sensorless control methods," *IEEE Trans. Ind. Appl.,* vol. 43, no. 4, pp. 990-1000, Jul./Aug. 2007.
[9] Zhu, Z.Q, et al., "Investigation of effectiveness of sensorless operation in carrier-signal-injection-based sensorless-control methods," *IEEE Trans. Ind. Electron.,* vol.58, pp. 3431-3439, 2011.
[10] S.C. Yang, et al., "Surface permanent magnet synchronous machine design for saliency tracking self-sensing position estimation at zero and low speeds," *IEEE Trans. Ind. Appl.,* vol. 47, no. 5, pp. 2103-2116, 2011.
[11] Xin Luo, et al., "PMSM Sensorless Control by Injecting HF Pulsating Carrier Signal Into Estimated Fixed-Frequency Rotating Reference Frame", *IEEE Trans. Ind. Electron.,* vol. 63, pp. 2294-2303, 2016.
[12] Ravikumar Setty. A, et al., "Comparison of high frequency signal injection techniques for rotor position estimation at low speed to standstill of PMSM*" India International Conference on Power Electronics (IICPE),* 2012.
[13] P. L. Xu and Z. Q. Zhu, "Comparison of carrier signal injection methods for sensorless control of PMSM drives", *Energy Conversion Congress and Exposition (ECCE),* pp. 5616-5623, 2015.
[14] J. Holtz, "Acquisition of position error and magnet polarity for sensorless control of PM synchronous machines," *IEEE Trans. Ind. Appl.,* vol. 44, no. 4, pp. 1172–1180, 2008.
[15] Andrew S, et al., "Inverter Device Nonlinearity Characterization Technique for Use in a Motor Drive System,"*IEEE Trans. Ind. Appl.,* vol. 51, pp. 2331-2339, 2015.
[16] Gaolin Wang, et al., "Self-Commissioning of Permanent Magnet Synchronous Machine Drives at Standstill Considering Inverter Nonlinearities," *IEEE Trans. Power Electron.,* vol. 29, pp. 6615-6627, 2014.
[17] Yi Li, et al., "Improved Rotor-Position Estimation by Signal Injection in Brushless AC Motors, Accounting for Cross-Coupling Magnetic Saturation", *IEEE Trans. Ind. Appl.,* vol.45, no.5, pp.1843-1849, 2009.
[18] M. Moghadam and F. Tahami, "Sensorless control of PMSMs with tolerance for delays and stator resistance uncertainties," *IEEE Trans. Power Electron.,* vol. 28, no. 3, pp. 1391–1399, Mar. 2013.
[19] A. Piippo, et al., "Adaptation of motor parameters in sensorless PMSM drives," *IEEE Trans. Ind. Appl.,*vol. 45, no. 1, pp. 203–212, Jan. 2009.
[20] Y. Inoue, et al., "Performance improvement of sensorless IPMSM drives in a low-speed region using online parameter identification," *IEEE Trans. Ind. Appl.,*vol. 47, no. 2, pp. 798–804, Mar. 2011.
[21] Sami Zaim, et al., "Robust Position Sensorless Control of Nonsalient PMSM at Standstill and Low Speeds" *IEEE Journal Of Emerging and Selected Topics in Power Electron.,* vol.2, no.3, pp. 640-650, Sep.2014.
[22] S. Y. Kim, et al., "An improved rotor position estimation with vector-tracking observer in PMSM drives with low-resolution Hall-effect sensors," *IEEE Trans. Ind. Electron.,* vol. 58, no. 9, pp. 4078– 4086, Sep. 2011.
[23] "Synchronous Servo Motors,"Parker Automation
Available:https://www.parkermotion.com/manuals/Hauser/HDY_HJ.pdf, [Accessed: DEC. 30, 2016].
[24] "Synchronous Servo Motors,"Kollmorgen
Available: http://www.kollmorgen.cn/zh-cn/products/motors/servo/akm-series/_literature/akm_selection_guide_en-us_revb/ [Accessed: DEC. 30, 2016].
[25] O. BelHadj Brahim, et al., "Continuous HFSI Technique Applied to Rotor Position Estimation of IPMSM at Standstill and Low Speed-A Survey", *IEEE, 8th International MultiConference on Systems, Signals & Devices,* SSD'11, pp. 1–10, March 2011.
[26] Ravikumar Setty, A. et al., "Compensation of rotor position estimation error due to stator winding resistance in signal injection based sensor less PMSM drives" *IEEE International Symposium on Sensorless Control for Electrical Drives (SLED),* Munich, Germany,17-19 Oct. 2013.